J. Membrane Biol. 141, 69–82 (1994)

The Journal of
Membrane
Biology

Maxi K^+ Channels on Human Vas Deferens Epithelial Cells

Y. Sohma[1]*, A. Harris[2], C.J.C. Wardle[2], M.A. Gray[1], B.E. Argent[1]

[1]Department of Physiological Sciences, University Medical School, Framlington Place, Newcastle upon Tyne NE2 4HH, United Kingdom
[2]Paediatric Molecular Genetics, Institute of Molecular Medicine, The John Radcliffe Hospital, Headington, Oxford, OX3 9DU, United Kingdom

Received: 29 November 1993/Revised: 17 March 1994

Abstract. The vas deferens forms part of the male reproductive tract and extends from the cauda epididymis to the prostate. Using the patch clamp technique, we have identified a Ca^{2+}-activated, voltage-dependent, maxi K^+ channel on the apical membrane of epithelial cells cultured from human fetal vas deferens. The channel had a conductance of ~250 pS in symmetrical 140 mM K^+ solutions, and was highly selective for K^+ over Na^+. Channel activity was increased by depolarization and by an elevation of bath (cytoplasmic) Ca^{2+} concentration, and reduced by cytoplasmic Ba^{2+} (5 mM) but not by cytoplasmic TEA (10 mM). Channel activity was also dependent on the cation bathing the cytoplasmic face of the membrane, being higher in a Na^+-rich compared to a K^+-rich solution. We estimated that up to 600 maxi K^+ channels were present on the apical membrane of a vas cell, and that their density was 1–2 per μ^2 of membrane. Activity of the channel was low on intact cells, suggesting that it does not contribute to a resting K^+ conductance. However, fluid in the lumen of the human vas deferens has a high K^+ concentration and we speculate that the maxi K^+ channel could play a role in transepithelial K^+ secretion.

Key words: Human vas deferens — Epithelium — Apical membrane — Maxi K^+ channels — Patch clamp — K^+ secretion

Introduction

The vas deferens forms the distal part of the excurrent duct system of the male reproductive tract and receives fluid and spermatozoa from the epididymis and transmits them distally to the urethra. Sperm maturation takes place within the excurrent duct system, and one function of the epithelia that line the epididymis and vas deferens is to create the correct luminal environment for this process to occur. Although the vas deferens has not been studied in detail, the epididymis is known to be a complex epithelium which can both absorb and secrete ions, water and macromolecules [17, 42].

One striking feature of the luminal fluid within the excurrent duct system of the male reproductive tract is its very high potassium content. Micropuncture studies have shown that the concentration of K^+ in the lumen of the rat vas deferens is 51.9 mM, i.e., about 11-fold higher than the plasma value [26]. Quantitatively, similar results have been observed for the K^+ concentration in luminal fluid isolated from the vas deferens of ram, boar, bull and hamster [*see* Fig. 4 in ref. 38]. The K^+ concentration in fluid obtained from human vas deferens during vasectomy operations was reported to be 111 mM [16]. This high K^+ concentration is no doubt largely produced by the absorption of water in the seminiferous tubules and the epididymis [26, 44]. However, the transepithelial potential in the rat vas deferens is −27 mV (lumen negative), and K^+ is above electrochemical equilibrium in the ductal fluid, suggesting that the ion must be actively secreted [26]. Direct evidence for K^+ secretion in the male reproductive tract has been provided by in vivo microperfusion studies on the rat epididymis [44] and by ^{86}Rb flux studies on cultured rat epididymal cell monolayers [9]. The high K^+ concentration in semen inhibits sperm motility and is necessary to maintain sperm quiescent during storage in the male reproductive tract [43].

The aim of this study was to investigate the mechanism by which K^+ could be secreted by the human vas deferens. K^+ secretion by the vas is likely to involve

* *Present address:* Department of Physiology, Osaka Medical College, Takatsuki Osaka 569, Japan

Correspondence to: B.E. Argent

an apical K^+ channel and in this respect it is interesting to note that calcium-activated, voltage-sensitive, maxi K^+ channels whose activity can be regulated by adrenaline [18], and also smaller conductance K^+ channels [5], are known to be present on the apical membrane of rat epididymal cells. Therefore, we set out to identify and characterize the K^+ channels in the apical membrane of human vas cells. Our results show that the predominant channel on this membrane is a Ca^{2+}-activated, voltage-dependent, maxi K^+ channel and we speculate that this channel is involved in transepithelial K^+ secretion by the human male reproductive tract. Some of our observations have been reported in preliminary form [31].

Materials and Methods

Human Vas Deferens Cell Culture

Primary monolayers of vas deferens cells were grown on glass coverslips from explants of second trimester human fetal vas deferens as previously described [15]. Six normal fetuses, and one fetus with Zellweger's syndrome, were obtained within 48 hr from mid-trimester prostaglandin-induced terminations or spontaneous abortions. Once established, two cell types predominate in the cultures; a large angular cell that does not appear tightly packed even in confluent areas, and a relatively small "cobblestone" cell that always appears in tightly packed colonies. Both cell types have been identified as epithelial cells on the basis of morphological, biochemical and immunocytochemical evidence [15].

The cultures were passaged on glass coverslips (passage numbers were between 1 and 12), and 2–4 days later sent from Oxford to Newcastle upon Tyne. After arrival in Newcastle, they were incubated for one to seven days in the standard growth medium [15] minus cholera toxin before electrophysiological studies were performed.

Electrophysiology

We studied a total of 117 coverslip cultures (between 2 and 34 coverslips from each of the seven fetuses). Single channel recordings were made at 21–23°C using the patch clamp technique [14]. All patches were obtained from the upper surface of small "cobblestone" cells in confluent areas of the monolayers. Full details of the electrophysiological techniques used in this study are described elsewhere [12]. The tissue bath was grounded, and potential difference across excised, inside-out patches (V_m) was referenced to the extracellular face of the membrane. Junction potentials were measured using a flowing 3M-KCl electrode [11], and the appropriate corrections were applied to our data.

In the cell-attached configuration, the potential difference across the patch is equal to the cell membrane potential (V_m) minus the pipette potential (V_p). Since the membrane potential is unknown in this configuration, we usually quote V_p values. However, to enable comparison of cell-attached *I/V* plots from different cells, and to cancel the effect of changes in V_m on channel activity, we have calculated V_m values as follows.

For a K^+-rich pipette solution and a Na^+-rich bath solution:

$$V_m = V_p - E_{rev} \tag{1}$$

where E_{rev} is the single channel current reversal potential in a Na^+-rich bath solution.

For Na^+-rich pipette and bath solutions:

$$V_m = V_p - E_{rev}^{\text{Na bath, K pipette}} \tag{2}$$

where $E_{rev}^{\text{Na bath, K pipette}}$ is the mean reversal potential measured with a Na^+-rich bath solution and a K^+-rich pipette solution (−61.3 mV, *see* Results).

Outward current, the flow of positive charge from the inside to the outside of the membrane, is indicated as an upward deflection on all the records. Conductance and reversal potential data were obtained from linear current/voltage (*I/V*) plots by least squares regression analysis.

To determine open state probability (P_o), mean open time (MOT) and mean closed time (MCT), current records were digitized at 5–10 kHz using a CED 1401 interface (Cambridge Electric Design, UK) and analyzed using a two-threshold transition algorithm which used a 50% threshold crossing parameter to detect events. P_o was calculated as the fraction of total time that channels were open using a minimum of 60 sec of data. When multi-channel patches were used for these determinations, we assumed that the total number of channels present was equal to the maximum number of simultaneous current transitions. MOT and MCT refer to the average open and closed times of the channel, respectively. To test whether individual channels in multi-channel patches operated independently of one another, the binomial theorem was used [4]:

$$P(n) = {}_N C_n p^n (1 - p)^{N-n} \tag{3}$$

Where N is the number of channels, p is open probability, and $P(n)$ is the probability of simultaneous opening of n channels. Because P_o was often very low in cell-attached patches it was not possible to estimate the number of channels (N) in the patch. Therefore, we usually quote NP_o values in this recording configuration.

Open (t_o) and closed (t_c) time constants were derived from a kinetic analysis of the same recordings that were analyzed to obtain the P_o, MOT and MCT data. Open and closed time distributions were fitted by the sum of two exponentials using least squares regression analysis. The curve-fitting algorithm disregarded channel events briefer than 200 μsec.

P_o/V_m data obtained from inside-out patches at each bath Ca^{2+} concentration were fitted by the Boltzmann curve as described below, using least squares regression analysis. For high P_o data (2 mM, 10, 3 and 1 μM Ca^{2+} in the bath):

$$P_o = P_{max}(1 + \exp[\alpha F(V_o - V_m)/RT])^{-1} \tag{4}$$

for low P_o data (1, 0.3 and 0.1 μM Ca^{2+} in the bath):

$$P_o = (1 + \exp[\alpha F(V_o - V_m)/RT])^{-1} \tag{5}$$

where F, R and T have their usual meanings, P_{max} is the maximum P_o value, V_m is the membrane potential tested, V_o is the membrane potential at which P_o is half-maximal, and α is the equivalent number of charges moving across the transmembrane potential during an open-close transition (the gating charge or Boltzmann constant) [24]. Some NP_o/V_m data were also analyzed using this approach.

Solutions and Chemicals

The Na^+-rich, extracellular-type, solution had the following composition (in mM): 138 NaCl, 4.5 KCl, 2 $CaCl_2$, 1 $MgCl_2$, 5 glucose, 10

N-2-hydroxyethylpiperazine-*N'*-2-ethanesulfonic acid (HEPES) at pH 7.4. The K^+-rich, intracellular-type, solution contained (in mM): 140 KCl, 2 $CaCl_2$, 1 $MgCl_2$, 5 glucose, 10 HEPES at pH 7.4. For some experiments, the Ca^{2+} concentration in these solutions was stabilized using a buffer system which contained 2 mM ethyleneglycol-*bis*-(β-aminoethylether)-*N,N'*-tetraacetic acid (EGTA) and variable amounts of $CaCl_2$ and $MgCl_2$. The free divalent cation concentrations in these solutions were calculated using the EQCAL program (Biosoft, Cambridge, UK), and were either 0.1, 0.3, 1, ~3 or ~10 μM for Ca^{2+}, and 1 mM for Mg^{2+}. Note that the buffering capacity of EGTA is weak at pH 7.4 when $[Ca^{2+}]$ is greater than 1 μM so the 3 and 10 μM Ca^{2+} buffers will not be accurate. When these solutions were used in the pipette, the Ca^{2+} concentration was always 1 μM and glucose was omitted. Pipette solutions were filtered through a 0.2 μM membrane filter before use.

All chemicals were purchased from commercial sources and were of the highest purity available.

Statistics

Significance of difference between means was determined using Student's paired or unpaired *t*-test. The level of significance was set at $P \leq 0.05$. All values are expressed as mean ± SEM (number of observations).

Results

Maxi K^+ Channels in Excised, Inside-Out, Patches

Basic Characteristics

Figure 1*A* (*a* and *b*) and *B* shows single channel currents recorded from inside-out patches excised from the upper surface of epithelial cells cultured from human fetal vas deferens. In these experiments, the intracellular surface of membrane patches was bathed in solutions containing 2 mM Ca^{2+}, and the channels were open for most of the time at all membrane potentials tested. The most frequent closing event was a rapid flickering closure, although occasionally longer closures lasting tens of milliseconds were also observed. With a K^+-rich solution bathing the cytoplasmic face, and a Na^+-rich solution bathing the extracellular face of the membrane, there was a marked outward rectification of the single channel currents, and inward currents were not detected (Fig. 1*C*). Under these conditions, the reversal potential was more negative than −50 mV, indicating that the channel is predominantly K^+ selective since K^+ is the only ion present with a negative equilibrium potential. When the Na^+ and K^+ gradients were reversed, the channel currents exhibited inward rectification and the reversal potential was more positive than +60 mV (Fig. 1*C*). That switching the direction of the K^+ gradient has no effect on the *I/V* plot, other than changing the direction of rectification, implies that the channel is equally K^+ selective in both directions of ion flow. When membrane patches were bathed in symmetrical K^+-rich solutions, the *I/V* relationship was linear, reversed at $V_m = 0.85 \pm 0.35$ mV, and the single channel conductance was 251 ± 8.7 pS ($n = 21$ patches) (Fig. 1*D*). Taken together, these data identify the channel as a maxi K^+ channel.

Maxi K^+ channels were present in 47.8% (424/887) of excised patches obtained from the upper surface of human vas cells, and more than 50% of these patches contained more than two channels (Fig. 2*A*). Occasionally, patches with up to 10–15 channels were obtained. The average number of channels in channel-containing patches was 1.2. Figure 2*B* shows a typical current trace obtained from an inside-out patch with five maxi K^+ channels, and Fig. 2*C* the current amplitude histogram obtained from this patch. Note that the six peaks on the histogram are well fitted by a Gaussian distribution. Figure 2*D* shows that the probability of finding a given number of channels in the open state is well described by the binomial theorem. Taken together, these data indicate that the maxi K^+ channels in this patch were opening and closing independently of one another.

Effects of Voltage and Ca^{2+} on Channel Activity

When the cytoplasmic face of the membrane was exposed to 2 mM Ca^{2+}, P_o remained over 0.8 at membrane potentials between +80 and −30 mV, but decreased sharply at more hyperpolarizing potentials (Fig. 3*A*). Figure 3*B* and 3*C* shows semilog plots of the mean open time (*MOT*), and mean closed time (*MCT*) as a function of the membrane potential (V_m). Membrane hyperpolarization decreased MOT and increased MCT (Fig. 3*B* and *C*). There was an approximately constant decrease in log MOT over the potential range tested; however, log MCT increased sharply at the more negative potentials. The minimal value of MCT was about 0.5 msec at membrane potentials around 0 mV; however, at potentials greater than +50 mV, MCT was sometimes increased due to the appearance of long closed periods in the current records (Fig. 3*C*).

Figure 4 shows the open time and closed time distributions obtained from an inside-out patch exposed to 2 mM Ca^{2+} on the cytoplasmic face of the membrane. Two exponentials are needed to describe these open and closed time distributions. In four experiments performed on separate patches at $V_m = -60$ mV ($P_o = 0.74 \pm 0.03$), the fast (t_{o1}) and slow (t_{o2}) time constants of the open time distribution were 0.31 ± 0.04 and 3.08 ± 0.58 msec, respectively, while the equivalent closed time constants, t_{c1} and t_{c2}, were 0.21 ± 0.02 and 1.88 ± 0.29 msec, respectively. These data indicate that the maxi K^+ channel has at least two open and two closed states.

The Table shows data from one patch in which the membrane potential has varied over the range 60 to

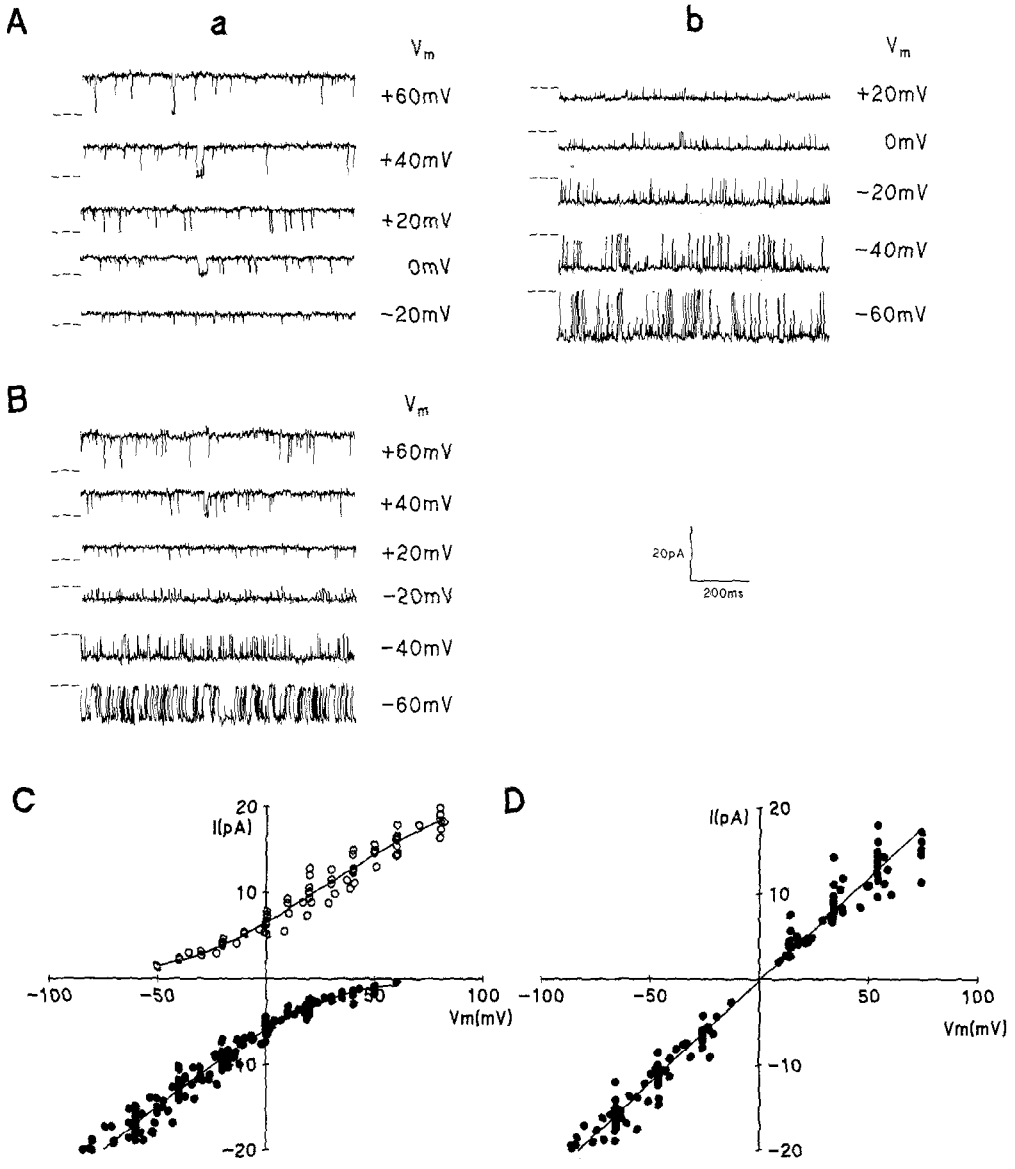

Fig. 1. Maxi K^+ channels in excised, inside-out, patches. (*A* and *B*) Typical single channel currents recorded at the membrane potentials (V_m) indicated to the right of each trace. Dashed lines indicate the closed state of the channel. Solutions: (*A,a*) pipette, Na^+-rich; bath, K^+-rich containing 2 mM Ca^{2+}. (*A,b*) Pipette, K^+-rich; bath, Na^+-rich containing 2 mM Ca^{2+}. (*B*) Pipette, K^+-rich; bath, K^+-rich containing 2 mM Ca^{2+}. Low-pass filtered at 3 kHz. (*C* and *D*) Single channel *I/V* plots. Solutions: (*C*) (○) pipette, Na^+-rich; bath, K^+-rich containing 2 mM Ca^{2+}. Data from nine patches. (●) Pipette, K^+-rich; bath, Na^+-rich containing 2 mM Ca^{2+}. Data from 28 patches. The lines were fitted by a third-order polynomial using least squares regression analysis. (*D*) (●) Pipette, K^+-rich; bath, K^+-rich containing 2 mM Ca^{2+}. Data from 21 patches. The line was fitted by least squares regression analysis.

−80 mV. This caused an 8.6-fold decrease in t_{o2}, whereas t_{c2} increased by a factor of 2.3. In contrast, the fast time constants, t_{o1} and t_{c1}, were hardly affected by changes in membrane voltage. Similar results were obtained in three additional experiments although the absolute values of the time constants varied markedly in different patches. These data indicate that the voltage-dependent changes in P_o, MOT and MCT of the maxi K^+ channel (*see* Fig. 3) are largely caused by changes in t_{o2} and t_{c2}.

Figure 5 shows the effect of quasi-physiological Ca^{2+} concentrations (3, 1 and 0.1 μM) on maxi K^+ channel activity in an inside-out patch. Lowering the bath Ca^{2+} concentration caused the appearance of long closed periods which reduced P_o (Fig. 5*A*). At the same time, channel opening became markedly voltage-dependent and the P_o/V_m relationship was shifted towards depolarizing potentials (Fig. 5*A* and *B*). However, there was no effect on the single channel *I/V* plot (Fig. 5*C*). Channel conductance in inside-out patches exposed to

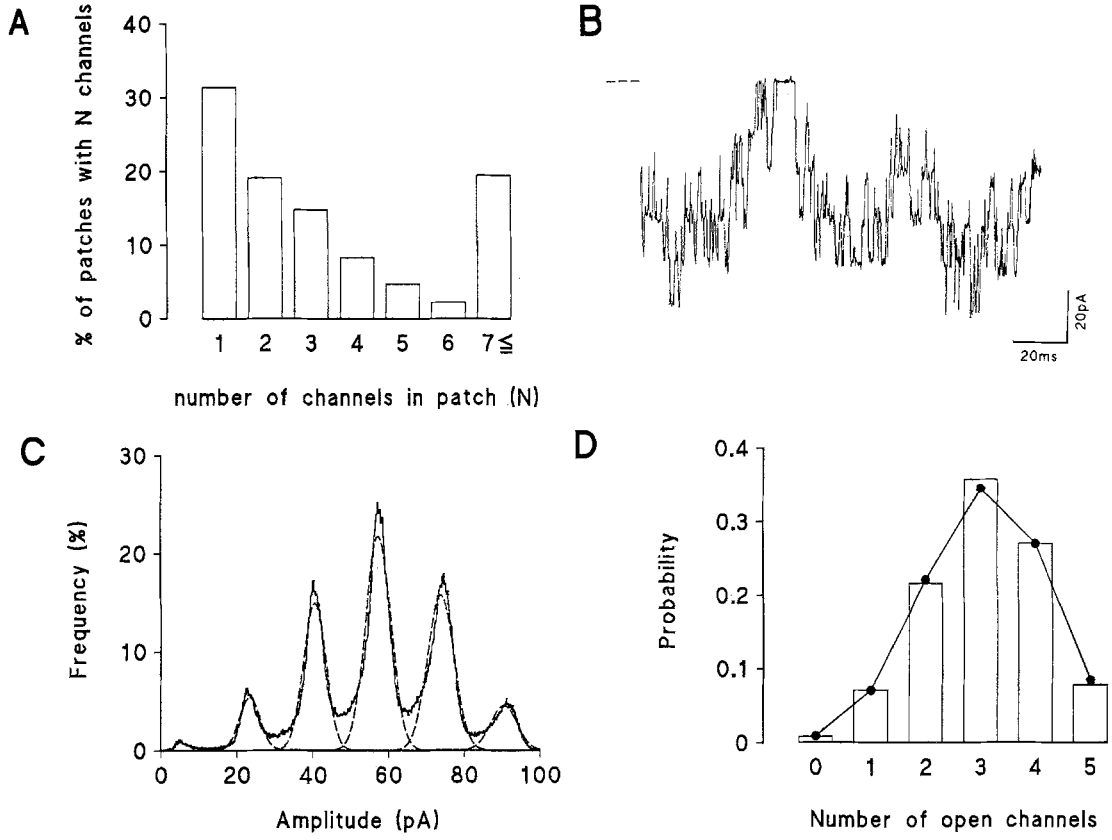

Fig. 2. Multiple maxi K^+ channels. (*A*) Number of channels in 424 channel-containing patches. The number of channels (*N*) in a patch was taken as the maximum number of simultaneous single channel current steps. (*B*) A typical current trace obtained from an inside-out patch bathed in symmetrical K^+-rich solutions containing 2 mM Ca^{2+} on the cytoplasmic face of the membrane. $V_m = -70$ mV. Low-pass filtered at 3 kHz. The dashed line shows current level when all channels are closed. (*C*) Current amplitude histogram derived by analysis of the current recording, including the data shown in *B*. Dashed lines are a Gaussian fit to the data. (*D*) Binomial analysis of open probabilities (closed circles, $N = 5$, $P = 0.6089$). Same data as *C*. Ordinate, probability of finding a given number of channels in the open state; abscissa, number of channels in the open state. The columns show the probabilities derived from the Gaussian curves in *C*.

0.1–3 μM Ca^{2+} was 257 ± 5.6 pS ($n = 30$) (Fig. 5*C*), which is not significantly different from the 251 ± 8.7 pS obtained with 2 mM Ca^{2+} on the cytoplasmic face of the membrane (Fig. 1*D*).

Figure 6 summarizes the effects of cytoplasmic Ca^{2+} (0.1–10 μM) and membrane potential on maxi K^+ channel activity. Lowering the bath Ca^{2+} concentration shifted the P_o/V_m curves towards depolarizing potentials (Fig. 6*A*), and increased V_O, the membrane potential required to give a P_o of 0.5 (Fig. 6*B*). However, the value of the gating charge (α, about 2.5), which determines the slope of the linear part of the P_o/V_m plot, was unaffected (Fig. 6*B*). This indicates that while lowering bath Ca^{2+} concentration shifts the P_o/V_m curves along the V_m axis, it has no remarkable effect on the steepness of the voltage dependence of P_o. When the cytoplasmic face of the membrane was exposed to 10 μM Ca^{2+}, the P_o/V_m relationship was similar to that observed in 2 mM Ca^{2+} (*compare* Figs. 6*A* and 3*A*). This suggests that over the potential range we tested, the effect of Ca^{2+} on P_o was essentially maximal at 10 μM.

Figure 6*C* and *D* shows semilog plots of MOT and MCT as a function of membrane potential at low bath Ca^{2+} concentrations (0.1 to 1 μM). These data reveal that the voltage dependence of the MCT is about 100 times larger than that of MOT when the bath Ca^{2+} concentration is lower than 1 μM. This suggests that the remarkable voltage dependency of P_o observed at submicromolar bath Ca^{2+} concentrations (Fig. 6*A*) is mainly the result of voltage-dependent changes in the duration of the closed state of the channel.

Effects of Cytoplasmic Na^+ and K^+ on Channel Activity

Figure 7*A* shows current recordings from an inside-out patch whose cytoplasmic face was exposed first to a K^+-rich solution and then to a Na^+-rich solution, both of

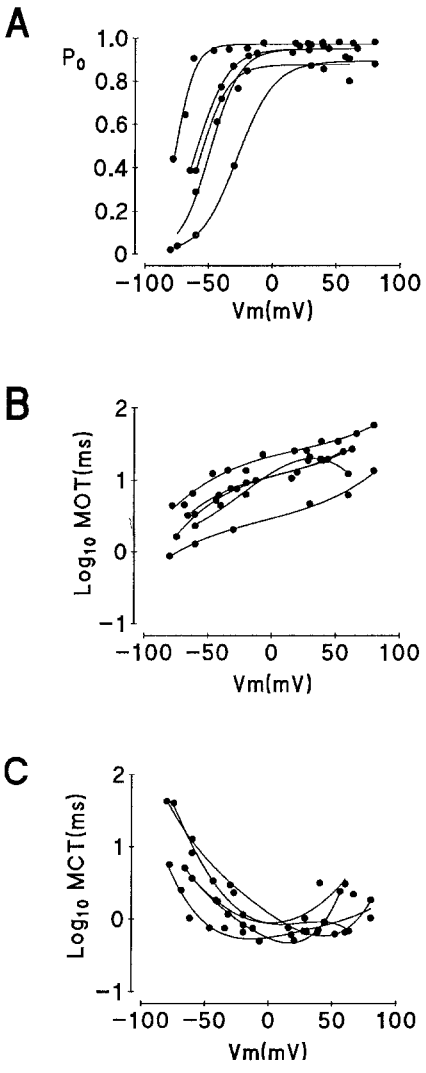

Fig. 3. Open state probability (P_o), mean open time (*MOT*), and mean closed time (*MCT*) of maxi K^+ channels in inside-out patches bathed in solutions containing 2 mM Ca^{2+} on the cytoplasmic face of the membrane. Solutions: (●) pipette and bath K^+-rich. (*A*) P_o. Data from five patches, three of which contained a single channel. Lines were fitted by Eq. (4) described in Materials and Methods using least squares regression analysis. (*B*) Semilog plot of MOT from five patches. (*C*) Semilog plot of MCT from five patches. The lines in *B* and *C* were fitted by third-order polynomial least squares regression analysis.

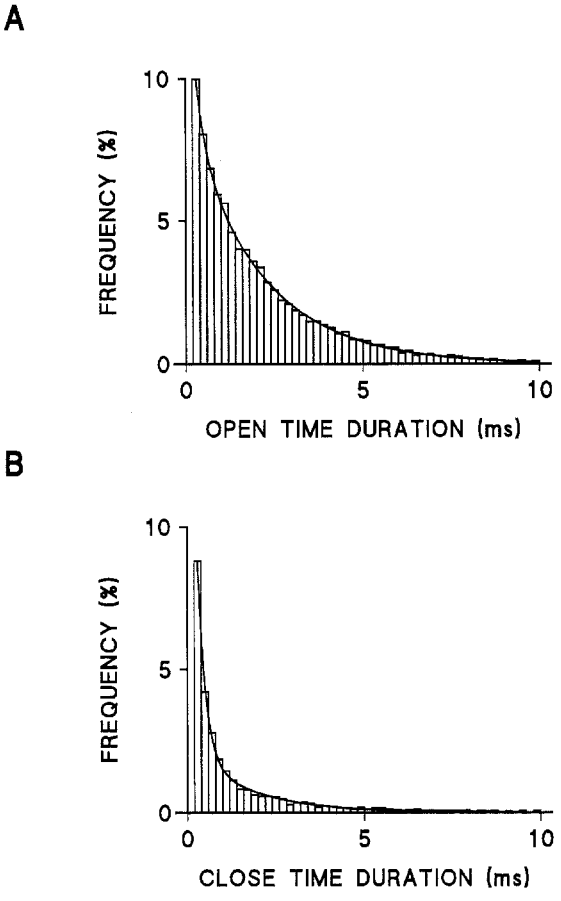

Fig. 4. Open time (*A*) and closed time (*B*) histograms for a maxi K^+ channel in an inside-out patch bathed in symmetrical K^+-rich solutions containing 2 mM Ca^{2+} on the cytoplasmic face of the membrane. V_m = −60 mV. Current recordings used for the analysis were filtered at 5 kHz and digitized at 10 kHz. Both distributions were best fit by the sum of two exponentials. In this particular experiment, the open time constants were t_{o1} = 0.29 and t_{o2} = 2.1 msec (amplitudes from y axis intercept of 6.8 and 8.7%, respectively; total number of events, 14,866), and the closed time constants t_{c1} = 0.22 and t_{c2} 1.8 msec (amplitudes of 26.8 and 2.2%, respectively; total number of events, 14,884). Representative of three other experiments.

which contained 2 mM Ca^{2+}. Note that channel activity was higher when the Na^+-rich solution was in the bath. This cannot be an artifact caused by channel rundown, because in this experiment the order of exposure was K^+ followed by Na^+. The effect of substituting bath Na^+ for K^+ on channel activity was fully reversible.

Figure 7*B* summarizes P_o data obtained from six patches that were exposed to both Na^+-rich and K^+-rich bath solutions. These data were well described by Eq. (4). P_{max}, V_o and α were 0.95 ± 0.01, −90.9 ± 5.7 and 2.2 ± 0.3, respectively, in the Na^+-rich bath solution, and 0.96 ± 0.01, −73.0 ± 2.0 and 2.2 ± 0.3, respectively, in the K^+-rich bath solution. There was a significant difference in V_o between K^+-rich and Na^+-rich bath solutions ($P < 0.05$, paired *t*-test), but no difference in either P_{max} or α. This indicates that the P_o/V_m curve was shifted along the V_m axis toward depolarizing potentials by the K^+-rich bath solution.

Figure 7*C* and *D* show semilog plots of MOT and MCT as a function of V_m in three single channel patches. At a V_m of −60 mV, MCT is clearly shorter when patches are bathed in a Na^+-rich as compared to a K^+-rich bath solution (Fig. 7*D*), but the MOT durations are similar at this potential (Fig. 7*C*). Thus, at V_m = −60 mV the higher P_o observed in a Na^+-rich bath solution

Table. Voltage dependence of t_{o1}, t_{o2}, t_{c1} and t_{c2}

V_m	t_{c1}		t_{c2}		t_{o1}		t_{o2}		P_o
mV	msec	(%)	msec	(%)	msec	(%)	msec	(%)	
60	0.21	(81.5)	1.55	(2.1)	0.79	(7.1)	22.20	(0.6)	0.98
40	0.14	(106.8)	0.88	(5.7)	0.38	(13.5)	8.48	(1.8)	0.95
20	0.17	(87.7)	0.94	(5.7)	0.37	(6.2)	8.38	(2.1)	0.94
−20	0.19	(71.1)	0.81	(8.0)	0.26	(4.4)	6.33	(3.0)	0.94
−40	0.17	(76.0)	0.77	(9.4)	0.49	(2.2)	6.37	(3.0)	0.95
−60	0.17	(63.0)	1.21	(7.7)	0.41	(3.8)	4.76	(3.9)	0.82
−80	0.35	(26.7)	3.55	(3.0)	0.55	(6.2)	2.57	(6.4)	0.49

The data were obtained from an inside-out patch bathed in symmetrical K^+-rich solutions containing 2 mM Ca^{2+} on the cytoplasmic face of the membrane. The current recordings were filtered at 5 kHz and digitized at 10 kHz. The probability amplitudes are indicated in parentheses.

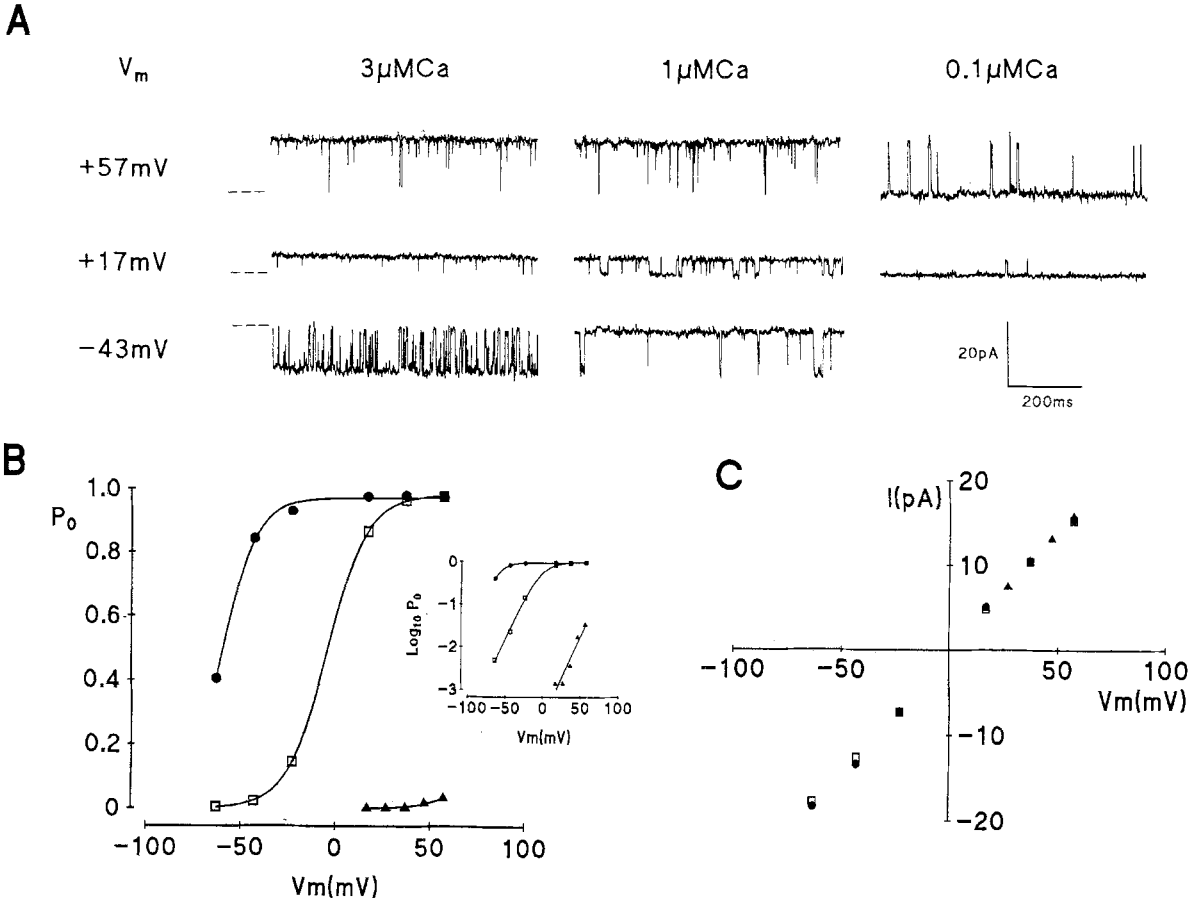

Fig. 5. Effects of quasi-physiological Ca^{2+} concentrations on a maxi K^+ channel in an excised, inside-out, patch. (*A*) Typical single channel currents recorded from a patch bathed in symmetrical K^+-rich solutions containing the indicated Ca^{2+} concentrations. Low-pass filtered at 3 kHz. (*B*) Effects of V_m on P_o of the maxi K^+ channel in the same patch. (●) 3, (□) 1 and (▲) 0.1 μM Ca^{2+} on the cytoplasmic face of the membrane. The lines for 3 and 1 μM Ca^{2+} were fitted by Eq. (4), and the line for 0.1 μM Ca^{2+} by Eq. (5) using least squares regression analysis (3 μM: $P_{max} = 0.97$, $V_o = -56.9$, $\alpha = 2.7$; 1 μM: $P_{max} = 0.98$, $V_o = -1.0$, $\alpha = 2.4$; 0.1 μM: $V_o = 95.8$, $\alpha = 2.4$). Inset shows a semilog plot of the same data. (*B*) Single channel *I/V* plots obtained from the current recordings, including the data shown in *A*.

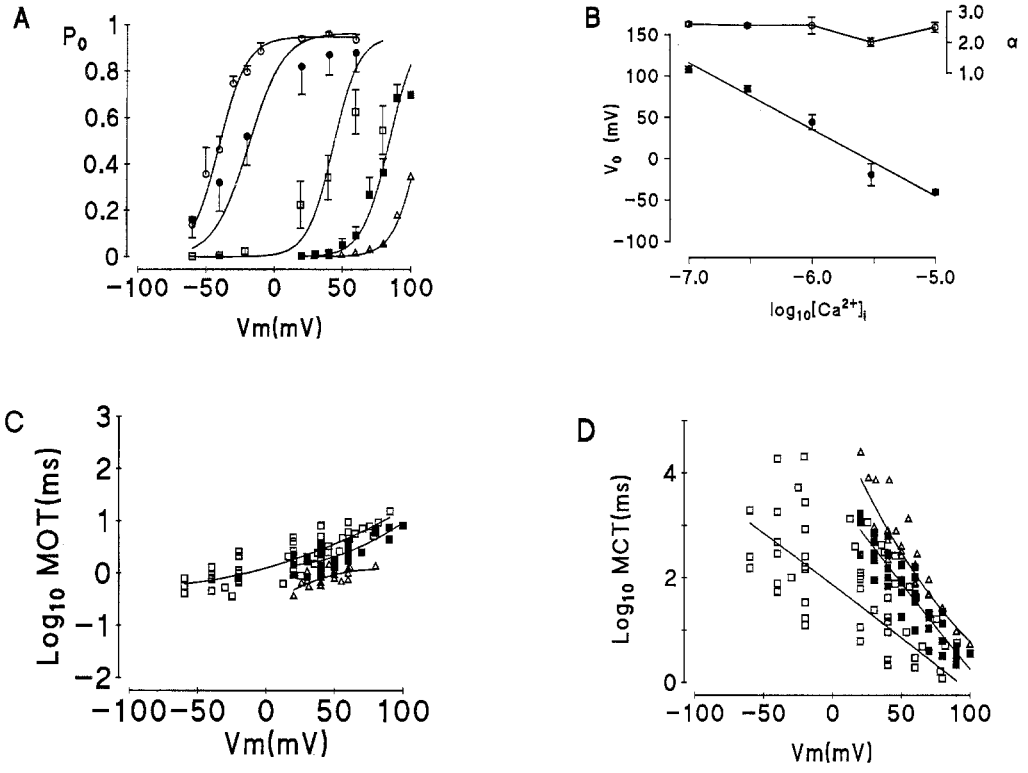

Fig. 6. Summary of the effects of quasi-physiological Ca^{2+} concentrations on P_o, MOT, and MCT of maxi K^+ channels in inside-out patches. Bath Ca^{2+} concentrations: 10 μM (○, n = 5), 3 μM (●, n = 7), 1 μM (□, n = 11), 0.3 μM (■, n = 7), 0.1 μM (△, n = 7). Solutions: pipette and bath K^+-rich. (*A*) Voltage dependence of P_o. The lines for 10 and 3 μM Ca^{2+} were fitted by Eq. (4) (10 μM: P_{max} = 0.95, V_o = −40.5, α = 2.5; 3 μM: P_{max} = 0.96, V_o = −18.8, α = 2.0). The lines for 1, 0.3 and 0.1 μM Ca^{2+} were fitted by Eq. (5) (1 μM: V_o = 43.3, α = 2.7; 0.3 μM: V_o = 84.5, α = 2.5; 0.1 μM: V_o = 108.1, α = 2.6). (*B*) Semilog plots of V_o and α against $[Ca^{2+}]_i$. The V_o data were fitted by Eq. (6) using least squares regression analysis. (*C*) Semilog plot of MOT at 1, 0.3 and 0.1 μM Ca^{2+}. (*D*) Semilog plot of MCT at 1, 0.3 and 0.1 μM Ca^{2+}. The lines in *C* and *D* were fitted by a third-order polynomial using least squares regression analysis.

is largely explained by a shorter MCT. However, as shown by the current tracings in Fig. 7*A* and the Log_{10} MOT *vs.* V_m plot in Fig. 7*C*, when V_m was hyperpolarized to −80 mV the MOT duration was also increased in a Na^+-rich bath solution. These data suggest that when the membrane is strongly hyperpolarized (i.e., to −80 mV) changes in both MCT and MOT may contribute to the higher P_o observed in a Na^+-rich as compared to a K^+-rich bath solution.

Effects of Ba^{2+} and TEA on Channel Activity

Figure 8 shows that application of 5 mM Ba^{2+} to the cytoplasmic face of the membrane blocked the maxi K^+ channel. Exposure to Ba^{2+} caused the appearance of long closing events and reduced P_o from 0.93 to 0.11 at V_m = 0 mV and from 0.92 to 0.65 at V_m = −40 mV, indicating that the block is voltage dependent. Similar results were obtained in two other experiments. In contrast, the application of 10 mM TEA^+ to the cytoplasmic face of the membrane had no effect on the activity of maxi K^+ channels at V_m values between −60 and +60 mV (n = 5, *data not shown*).

Maxi K^+ Channels in Cell-attached Patches

The single channel current traces shown in Fig. 9*A* were obtained from a cell-attached patch on the upper surface of a human vas cell with Na^+-rich solutions in both the pipette and bath. Channel openings were only observed at strongly depolarizing pipette potentials, and usually not at pipette potentials near 0 mV, i.e., close to the resting membrane potential of the cell. Similar results were obtained with a K^+-rich pipette solution.

Figure 9*B* illustrates typical *I/V* relationships for maxi K^+ channels in cell-attached patches. With Na^+-rich solutions in both pipette and bath, the single channel *I/V* plot showed marked outward rectification, and inward currents were not detected even at hyperpolarizing potentials. With a K^+-rich solution in the pipette, the cell-attached *I/V* relationship was essentially linear over the V_p range +20 to −100 mV (although some channels exhibited slight inward rectification at high depolarizing potentials, *see* Fig. 9*C*), and the reversal po-

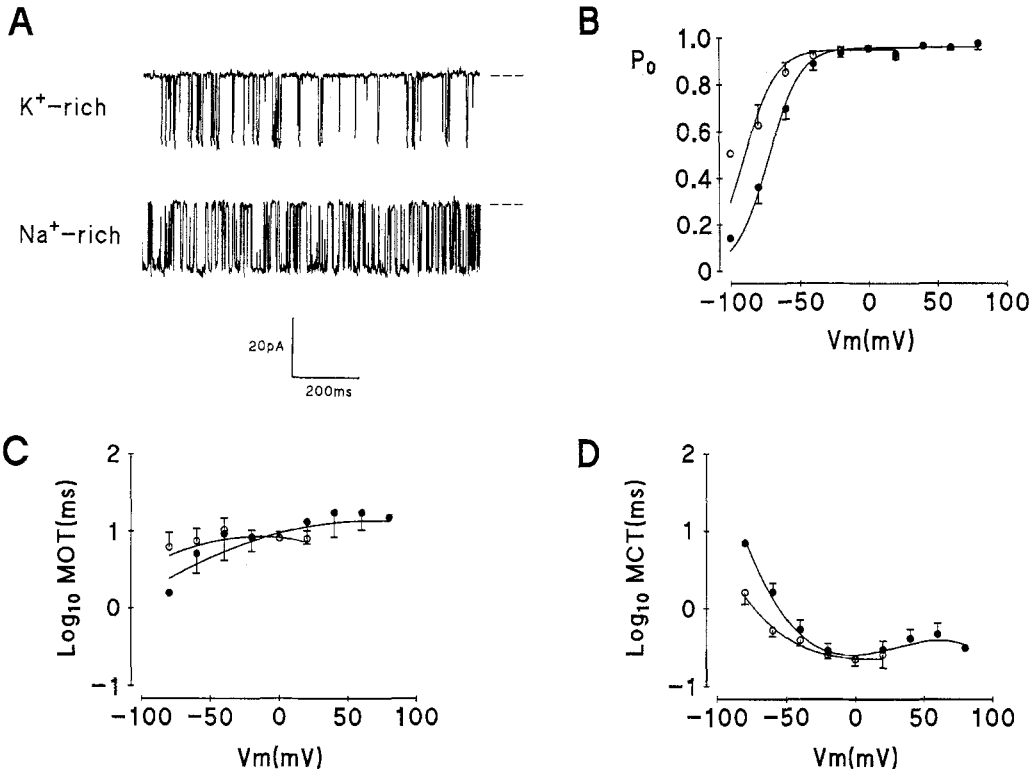

Fig. 7. Effects of Na^+ and K^+ on maxi K^+ channel activity. (*A*) Typical single channel currents recorded from an inside-out patch with K^+-rich and Na^+-rich solutions containing 2 mM Ca^{2+} in the bath. The pipette solution was K^+-rich. $V_m = -80$ mV. Low-pass filtered at 3 kHz. Paired data from the same patch. (*B, C* and *D*) (●) Pipette and bath K^+-rich. (○) Pipette, K^+-rich; bath, Na^+-rich. (*B*) P_o. Paired data from six patches. Lines were fitted using Eq. (4). (*C*) Semilog plot of MOT. Paired data from three patches. (*D*) Semilog plot of MCT. Paired data from three patches. The lines in *B* and *C* were fitted by a third-order polynomial using least squares regression analysis.

tential was −73.5 mV. Intracellular $[K^+]$ has not been measured in human fetal vas deferens epithelial cells; however, assuming pipette $[K^+]$ is close to intracellular $[K^+]$, the reversal potential determined under these conditions will be close to the membrane potential of the cells. The mean reversal potential in this series of experiments was -61.3 ± 3.4 mV ($n = 23$ patches).

Figure 9*C* and *D* shows all 25 cell-attached *I/V* plots obtained with a K^+-rich pipette solution, and the 5 obtained using a Na^+-rich solution. To allow a comparison of plots obtained from different cells, the voltage axis has been scaled as membrane potential (V_m) rather than pipette potential (V_p). With a K^+-rich solution in the pipette, the cell-attached single channel conductance was 236 ± 6.4 pS ($n = 24$ patches) (Fig. 9*C*). This value is not significantly different from the 257 ± 5.6 pS obtained for inside-out patches bathed in symmetrical K^+-rich solutions and exposed to 0.1–1 μM Ca^{2+} in the bath. With Na^+-rich pipette solutions, the *I/V* relationship in cell-attached patches was very similar to that obtained from inside-out patches with Na^+ in the pipette and K^+ in the bath. However, there was some inward rectification at membrane potentials more positive than +50 mV in cell-attached patches (*compare* Figs. 9*D* and 1*C*). Thus, at the higher depolarizing potentials, the current amplitude in cell-attached patches is smaller than that in inside-out patches at the same V_m. This rectification is probably due to voltage-dependent blockade of the maxi K^+ channel by intracellular Na^+ [*see* ref. 22].

Figure 10*A* shows the effects of membrane potential on the activity of maxi K^+ channels in cell-attached patches. P_o varied widely in different cells, but the voltage dependencies of P_o were similar, and like those observed in inside-out patches exposed to low Ca^{2+} bath solutions (shown by dashed lines in Fig. 10*A*). Comparisons of these cell-attached and inside-out patch data suggest that in most human vas cells the intracellular Ca^{2+} concentration is 0.1 μM or less (assuming channel regulatory mechanisms are identical *in situ* and in excised patches). Figure 10*B and* C are, respectively, semilog plots of MCT and MOT in cell-attached patches. As for P_o, the voltage dependencies of MOT and MCT are similar to those in inside-out patches bathed in low Ca^{2+} media (*compare* Figs. 10*B* and *C* with 6*C* and *D*). These data suggest that the kinetic behavior of maxi K^+ channels is similar in both cell-attached patches and excised, inside-out, patches.

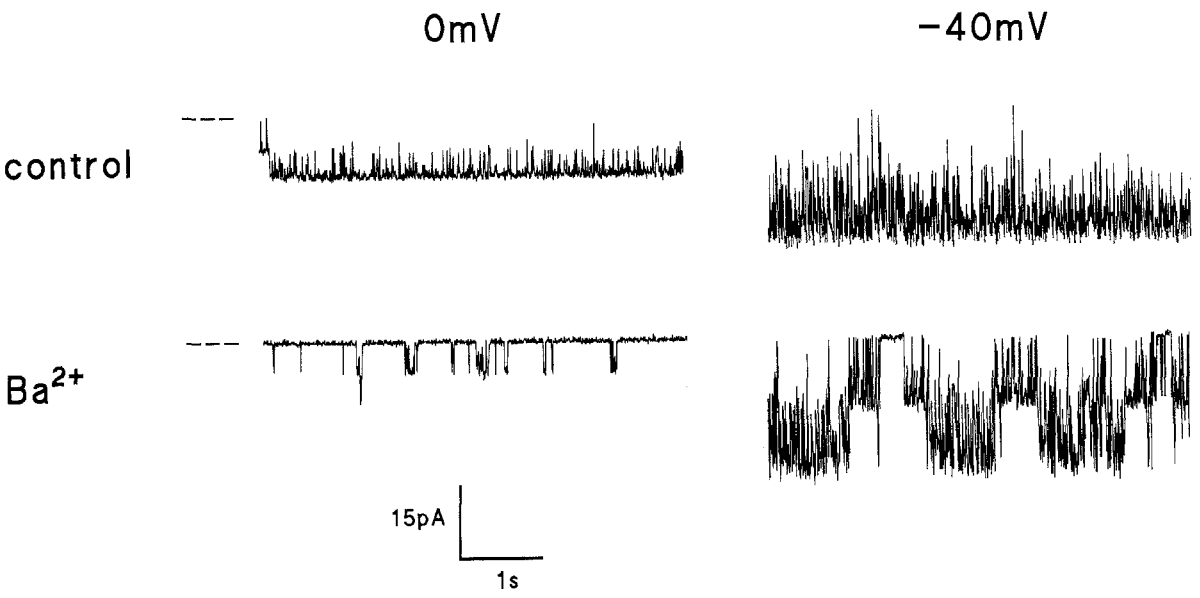

Fig. 8. Effects of Ba^{2+} on maxi K^+ channels in an inside-out patch. Ba^{2+} (5 mM) was added to the bath solution. Solutions: pipette, K^+-rich; bath, Na^+-rich containing 2 mM Ca^{2+}. Low-pass filtered at 3 kHz.

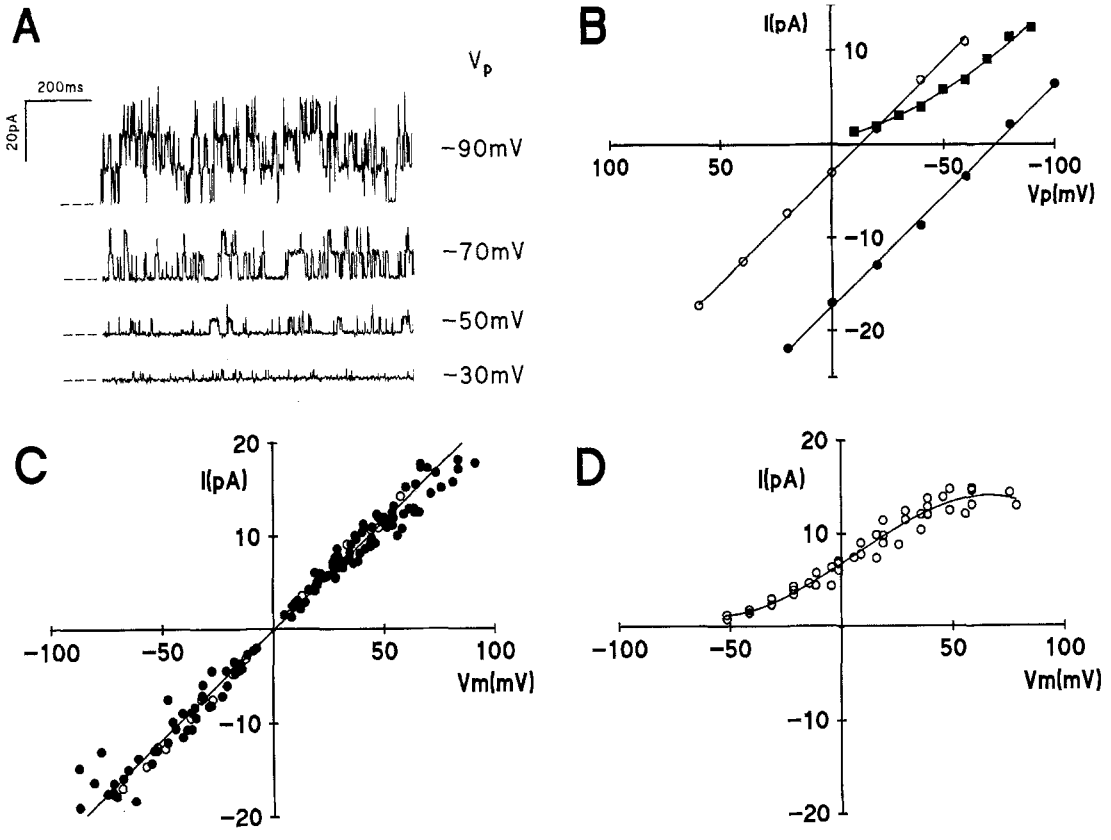

Fig. 9. Maxi K^+ channels in cell-attached patches. (*A*) Typical single channel currents recorded at pipette potentials (V_p) shown to the right of each trace. Low pass filtered at 3 kHz. Solutions: pipette, Na^+-rich; bath, Na^+-rich. (*B*) *I/V* plots. Solutions: (●) pipette, K^+-rich; bath, Na^+-rich. (○) Pipette and bath, K^+-rich. (■) Pipette, Na^+-rich; bath, Na^+-rich. (*C* and *D*) Summary of cell-attached *I/V* data. To facilitate comparison of *I/V* plots from different cells the voltage axis has been scaled as V_m instead of V_p. V_m was calculated as described in Materials and Methods. Solutions: (*C*) (●) pipette, K^+-rich; bath, Na^+-rich, 23 patches. (○) Pipette and bath K^+-rich, two patches. The line was fitted by least squares regression analysis. (*D*) (○) Pipette, Na^+-rich; bath, Na^+-rich, five patches. The line was fitted by a third-order polynomial using least squares regression analysis.

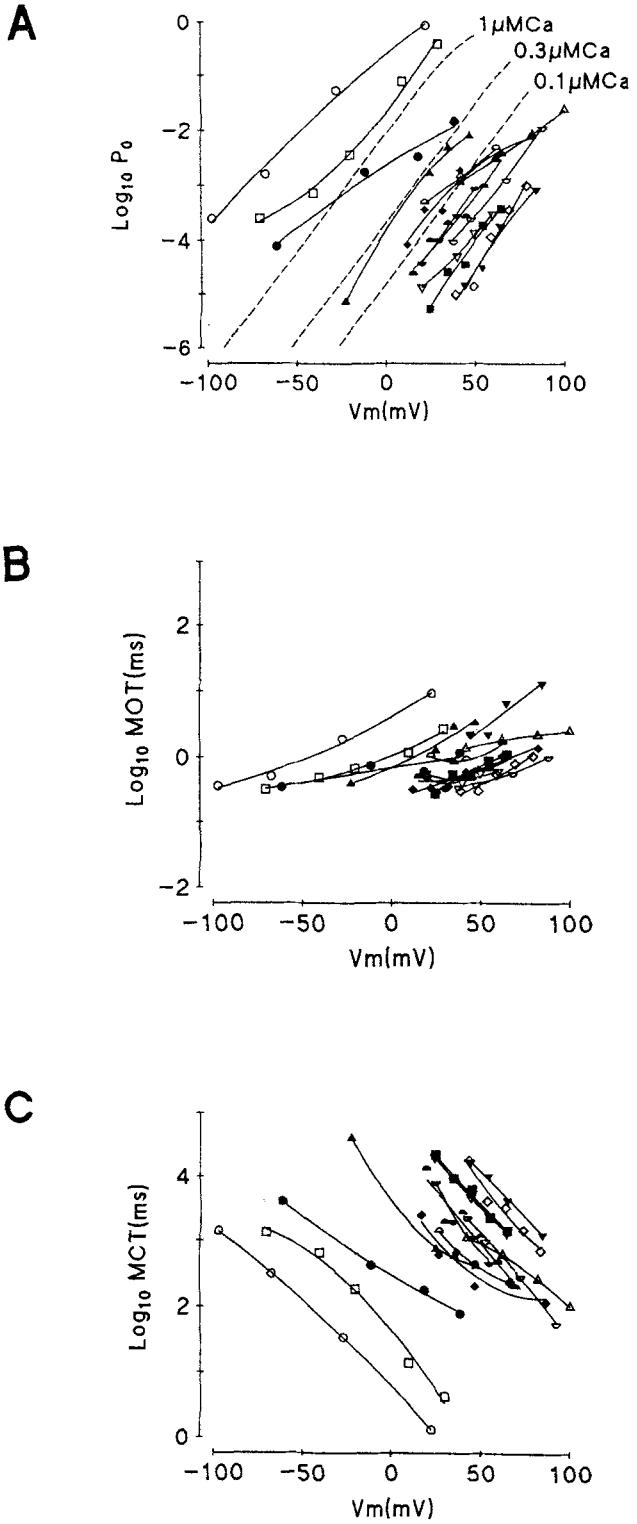

Fig. 10. Effects of V_m on the P_o, MOT and MCT of maxi K^+ channels in cell-attached patches. Data from 14 patches obtained from different cells. Each symbol represents a different cell. (*A*) Semilog plots of P_o. For comparison, the dashed lines show the P_o/V_m relationship for inside-out patches at the indicated bath Ca^{2+} concentrations (taken from Fig. 6*A*). (*B*) Semilog plot of MOT. (*C*) Semilog plot of MCT. All unbroken lines were fitted by a third-order polynomial using least squares regression analysis.

Discussion

Using the patch clamp technique, we have identified a large conductance K^+ channel on epithelial cells cultured from human fetal vas deferens. The channel had a conductance of about 250 pS in symmetrical 140 mM K^+ solutions, and is highly selective for K^+ over Na^+. Channel P_o was increased by depolarization and by an elevation of bath (cytoplasmic) Ca^{2+} concentration, and reduced by cytoplasmic Ba^{2+}. Taken together, these data identify the channel as a Ca^{2+}-activated, voltage-dependent, maxi K^+ channel [23].

Membrane hyperpolarization decreased the mean open time (MOT), and increased the mean closed time (MCT) of the vas maxi K^+ channel. Our kinetic analysis indicated that the channel has at least two open (t_{o1} and t_{o2}) and two closed states (t_{c1} and t_{c2}). With 2 mM Ca^{2+} bathing the cytoplasmic face of the membrane, the fast time constants, t_{o1} and t_{c1}, were hardly affected by changes in membrane potential. However, t_{o2} decreased 8.6-fold and t_{c2} increased 2.3-fold when the membrane potential was varied over the range 60 to −80 mV. These data indicate that voltage-dependent changes in channel P_o are largely caused by alterations in the duration of the slow time constants, t_{o2} and t_{c2}. In general, the kinetic properties of the human vas maxi K^+ channel appear similar to those of maxi K^+ channels previously identified in many other cell types. However, one new finding is that activity of the vas channel was higher with Na^+ compared to K^+ on the cytoplasmic face of the membrane. There were no cation-dependent differences in P_{max}, or the gating charge (α); however, switching from a Na^+-rich to a K^+-rich bath solution shifted the P_o/V_m relationship along the V_m axis towards depolarizing potentials, i.e., a stronger depolarization was required to produce a given P_o in K^+-rich compared to Na^+-rich bath solutions. This difference in P_o reflects that when the membrane was strongly hyperpolarized (i.e., −80 mV), MCT was longer and MOT was shorter in a K^+-rich compared to a Na^+-rich bath solution. A possible explanation for this phenomena is that K^+ and Ca^{2+} compete for the Ca^{2+} binding site on the maxi K^+ channel. However, additional experiments will be required to clarify this point.

Lowering the bath Ca^{2+} concentration to quasi-physiological levels also shifted the P_o/V_m relationship towards depolarizing potentials, while having no appreciable effect on the voltage dependence of P_o. We found that Ca^{2+} concentrations greater than 0.1 μM were required to significantly activate the vas cell maxi K^+ channel in excised patches. This contrasts with the effect of Ca^{2+} on the P_o of these channels in pig and guinea pig pancreatic acini [29, 36], the mandibular salivary gland [30], the lacrimal gland [7], and rat enterocytes [32]. In all these tissues, channel activity is detectable with 0.1 μM Ca^{2+} on the cytoplasmic face of the membrane, even at hyperpolarizing potentials, and

full activation occurs at voltages around +20 mV [7, 29, 30, 32]. In terms of its Ca^{2+} sensitivity, the human vas cell channel more closely resembles maxi K^+ channels in cultured skeletal muscle [1], choroid plexus [2, 3], pancreatic islet cells [8], and pancreatic duct cells [12].

Location and Density of the Maxi K^+ Channel

The maxi channel we studied was found in patches derived from the upper surface of cultured human vas deferens cells, suggesting that in vivo the channel may be located on the apical membrane of the epithelium. As yet, monolayer cultures of these human vas cells have not been reconstituted as polarized epithelia, and no patch clamp studies have been carried out on the intact epithelium, so we cannot be sure about the location of the channel. However, support for apical localization comes from the finding that maxi K^+ channels have also been identified in the apical membrane of polarized rat epididymal cell cultures [18].

We found maxi K^+ channels in 48% of excised patches derived from human vas cells, and on average each patch contained 1.2 channels. Assuming that ~1–2 μ^2 of membrane is excised by a thick-walled patch pipette, and that the apical surface area of the human vas cells averages about 500 μ^2 (determined from micrographs in ref. 15), it can be calculated that up to 600 channels could be present in the apical membrane.

Physiological Role of the Maxi K^+ Channel

The biophysical characteristics of the vas maxi K^+ channel were essentially similar in both cell-attached and excised patches. However, maxi K^+ channels in cell-attached patches were usually inactive at the resting membrane potential of the cell (i.e., at $V_p = 0$ mV). Thus, these channels may not contribute to the resting K^+ conductance of the vas cell, at least under the conditions we used in this study. Similar conclusions have been reached about the contribution of maxi K channels to the resting K^+ conductance in a number of other epithelial cell types [33, 39]. In preliminary experiments we have observed an increase in activity of the maxi K^+ channel following exposure of the human vas cells to either acetylcholine or cyclic AMP. However, the effect of these stimulants on maxi K^+ channel activity was very variable and probably indirect, i.e., caused by membrane depolarization following activation of a chloride conductance.

The physiological function of the epithelia that line the distal regions of the male reproductive tract (epididymis and vas deferens) is to generate the correct luminal environment for sperm maturation. In vivo these epithelia are normally absorptive, reabsorbing a major part of the testicular fluid [26, 44]. However, it has recently been shown that agonists which elevate intracellular cyclic AMP stimulate electrogenic chloride secretion and increase whole-cell chloride currents in both rat [19, 25, 40], and human [20] epididymal cells. This cyclic AMP-activated secretory chloride current is carried by CFTR chloride channels which have been identified in human epididymal cells [34]. It is possible that the maxi K^+ we have identified plays a role in chloride secretion by the vas deferens epithelium. The "classical" model of electrogenic chloride secretion places K^+ channels on the basolateral membrane [13, 35]; however, K^+ channels have been found in the apical membrane of some chloride-secreting epithelia [e.g., lacrimal acinar cells, ref. 37; and epididymis, refs. 5, 18], and an alternative model for chloride secretion, which involves activation of maxi K^+ and Cl^- channels on both apical and basolateral plasma membranes, has been proposed [28]. Furthermore, computer modeling of secretory cells has shown that placing 10–20% of the cellular K^+ conductance on the apical membrane will enhance a secretory mechanism driven by secondary active transport of chloride [6]. However, a role for apical maxi K^+ channels in chloride secretion by the male reproductive tract seems unlikely, since in rat epididymis apical application of barium (which blocks the channel, *see above*) does not inhibit electrogenic chloride secretion [41].

Alternatively, the maxi K^+ channel may be involved in K^+ secretion. This could occur in a two-stage process: first, K^+ would be pumped into the vas cell by a basolateral Na^+/K^+ ATPase, and then secreted into the lumen by passive diffusion down its electrochemical gradient. The concentration of K^+ in fluid sampled from the human vas deferens has been reported to be about 20-fold higher than the plasma value [16]. Furthermore, in the rat, K^+ is known to be accumulated above electrochemical equilibrium in the vas lumen, suggesting that active secretion of the ion takes place [26]. The idea that the maxi K^+ channel could play a role in this process is supported by channels (including maxi K^+ channels) having been identified in the apical membrane of K^+ secreting principal cells in the renal cortical collecting duct [10, 21, 27]. That activity of the vas maxi K^+ channel was so low on unstimulated cells implies that K^+ secretion by the male reproductive tract is likely to be a regulated process.

In conclusion, we have identified a maxi K^+ channel on human vas deferens epithelial cells. The channel is probably located on the apical plasma membrane of the vas cells and could provide a pathway for K^+ secretion into the lumen of the male reproductive tract.

Funded by grants from the Cystic Fibrosis Trust and the Medical Research Council (UK). We thank Mr. David Stephenson for excellent technical assistance.

References

1. Barrett, J.N., Magleby, K.L., Pallotta, B.S. 1982. Properties of single calcium-activated potassium channels in cultured rat muscle. *J. Physiol.* London **331:**211–230
2. Brown, P.D., Loo, D.D.F., Wright, E.M. 1988. Ca^{2+}-activated K^+ channels in the apical membrane of *Necturus* choroid plexus. *J. Membrane Biol.* **105:**207–219
3. Christensen, O., Zeuthen, T. 1987. Maxi K^+ channels in leaky epithelia are regulated by intracellular Ca^{2+}, pH and membrane potential. *Pfluegers Arch.* **408:**249–259
4. Colquhoun, D., Hawkes, H.G. 1981. On the stochastic properties of single ion channels. *Proc. R. Soc. London B* **211:**205–235
5. Cook, D.I., Huang, S.J., Wilson, S.M., Wong, P.Y.D., Young, J.A. 1989. Ion channels in the apical plasma membrane of the rat cauda epididymides. *J. Physiol.* **423:**57P
6. Cook, D.I., Young, J.A. 1989. Effect of K^+ channels in the apical plasma membrane on epithelial secretion based on secondary active Cl^- transport. *J. Membrane Biol.* **110:**139–146
7. Findlay, I. 1984. A patch-clamp study of potassium channels and whole-cell currents in acinar cells of the mouse lacrimal gland. *J. Physiol.* **350:**179–195
8. Findlay, I., Dunne, M.J., Petersen, O.H. 1985. High-conductance K^+ channel in pancreatic islet cells can be activated and inactivated by internal calcium. *J. Membrane Biol.* **83:**169–175
9. Fu, W.O., Huang, S.J., Wilson, S.M., Wong, P.Y.D. 1990. Adrenaline stimulates K^+ ($^{86}RB^+$) efflux across the apical and basolateral membranes of monolayer cultures of the rat epididymis. *J. Physiol.* **423:**50P
10. Gitter, A.H., Beyenbach, K.W., Christine, C.W., Gross, P., Minuth, W.W., Frömter, E. 1987. High-conductance K^+ channel in apical membranes of principal cells cultured from rabbit renal cortical collecting duct anlagen. *Pfluegers Arch.* **408:**282–290
11. Gray, M.A., Greenwell, J.R., Argent, B.E. 1988. Secretin-regulated chloride channel on the apical plasma membrane of pancreatic duct cells. *J. Membrane Biol.* **105:**131–142
12. Gray, M.A., Greenwell, J.R., Garton, A.J., Argent, B.E. 1990. Regulation of maxi-K^+ channels on pancreatic duct cells by cyclic AMP-dependent phosphorylation. *J. Membrane Biol.* **115:**203–215
13. Greger, R., Schlatter, E., Wang, F., Forrest, J.N. 1984. Mechanism of NaCl secretion in the rectal gland of spiny dogfish (*Squalus acanthias*). III. Effect of stimulation of secretion by cyclic AMP. *Pfluegers Arch.* **402:**376–384
14. Hamill, O.P., Marty, A., Neher, E., Sakmann, B., Sigworth, F.J. 1981. Improved patch-clamp techniques for high-resolution current recording from cells and cell-free membrane patches. *Pfluegers Arch.* **391:**85–100
15. Harris, A., Coleman, L. 1989. Ductal epithelial cells cultured from human foetal epididymis and vas deferens: relevance to sterility in cystic fibrosis. *J. Cell Sci.* **92:**687–690
16. Hinton, B.T., Pryor, J.P., Hirsh, A.V., Setchell, B.P. 1981. The concentration of some inorganic ions and organic compounds in the luminal fluid of the human ductus deferens. *Int. J. Androl.* **4:**457–461
17. Hinton, B.T., Turner, T.T. 1988. Is the epididymis a kidney analogue? *NIPS* **3:**28–31
18. Huang, S.J., Cook, D.I., Jones, A.O., Wong, P.Y.D., Young, J.A. 1990. The Ca^{2+}- and voltage-sensitive potassium channels in the rat epididymis. *In:* Exocrine Secretion II. P.Y.D. Wong and J.A. Young, editors, pp. 65–68
19. Huang, S.J., Fu, W.O., Chung, Y.W., Zhou, T.S., Wong, P.Y.D. 1993. Properties of cAMP-dependent and Ca^{2+}-dependent whole-cell Cl^- conductances in rat epididymal cells. *Am. J. Physiol.* **264:**C794–C802
20. Huang, S.J., Leung, A.Y.H., Fu, W.O., Chung, Y.W., Zhou, T.S., Chan, P.S.F., Wong, P.Y.D. 1992. Electrophysiological studies of anion secretion in cultured human epididymal cells. *J. Physiol.* **455:**455–469
21. Hunter, M., Lopes, A.G., Boulpaep, E., Giebisch, G. 1986. Regulation of single potassium ion channels from apical membrane of rabbit collecting tubule. *Am. J. Physiol.* **251:**F725–F733
22. Kawahara, K., Hunter, M., Giebisch, G. 1990. Calcium-activated potassium channels in the luminal membrane of *Amphiuma* diluting segment: voltage-dependent block by intracellular Na^+ upon depolarisation. *Pfluegers Arch.* **416:**422–427
23. Latorre, R., Miller, C. 1983. Conduction and selectivity in potassium channels. *J. Membrane Biol.* **71:**11–30
24. Latorre, R., Vergara, C., Hidalgo, C. 1982. Reconstitution in planar lipid bilayers of Ca^{2+}-dependent K^+ channel from transverse tubule membranes isolated from rabbit skeletal muscle. *Proc. Natl. Acad. Sci. USA* **79:**805–809
25. Leung, A.Y.H., Wong, P.Y.D. 1992. Studies of transepithelial Cl^- transport in cultured cauda epididymal cells of rats by the short-circuit current method. *J. Physiol. London* **457:**391–406
26. Levine, N., Marsh, D.J. 1971. Micropuncture studies of the electrochemical aspects of fluid and electrolyte transport in individual seminiferous tubules, the epididymis and the vas deferens in rats. *J. Physiol. London* **213:**557–570
27. Ling, B.N., Hinton, C.F., Eaton, D.C. 1991. Potassium permeable channels in primary cultures of rabbit cortical collecting tubule *Kidney Int.* **40:**441–452
28. Marty, A., Tan, Y.P., Trautmann, A. 1984. Three types of calcium-dependent channel in rat lacrimal glands. *J. Physiol.* **357:**293–325
29. Maruyama, Y., Petersen, O.H., Flanagan, P., Pearson, G.T. 1983. Quantification of Ca^{2+}-activated K^+ channels under hormonal control in pig pancreas acinar cells. *Nature* **305:**228–232
30. Maruyama, Y., Gallacher, D.V., Petersen, O.H. 1983. Voltage and Ca^{2+}-activated K^+ channel in baso-lateral acinar cell membranes of mammalian salivary glands. *Nature* **302:**827–829
31. Mathews, C.J., Sohma, Y., Harris, A., Chambers, J.A., Argent, B.E. 1992. Maxi-K^+ channels on epithelial cells cultured from human fetal vas deferens. *J. Physiol.* London **452:**344P
32. Morris, A.P., Gallacher, D.V., Lee, J.A.C. 1986. A large conductance, voltage- and calcium-activated K^+ channel in the basolateral membrane of rat enterocytes. *FEBS Lett.* **206:**87–92
33. Plant, S., Gray, M.A., Argent, B.E. 1992. K^+ channels on rat pancreatic duct cells *in vitro*. *J. Physiol.* **452:**360P
34. Pollard, C.E., Harris, A., Coleman, L., Argent, B.E. 1991. Chloride channels on epithelial cells cultured from human fetal epididymis. *J. Membrane. Biol.* **124:**275–284
35. Silva, P., Stoff, J., Field, M., Fine, L., Forrest, J.N., Epstein, F.H. 1977. Mechanism of active chloride secretion by shark rectal gland: role of Na-K-ATPase in chloride transport. *Am. J. Physiol.* **233:**F298–F306
36. Suzuki, K., Petersen, O.H. 1988. Patch-clamp study of single-channel and whole-cell K^+ currents in guinea pig pancreatic acinar cells. *Am. J. Physiol.* **255:**G275–G285
37. Tan, Y.P., Marty, A., Trautmann, A. 1992. High density of Ca^{2+}-dependent K^+ and Cl^- channels on the luminal membrane of lacrimal acinar cells. *Proc. Natl. Acad. Sci. USA* **89:**11229–11233
38. Turner, T.T., Hartmann, P.K., Howards, S.S. 1977. In vivo sodium, potassium, and sperm concentrations in the rat epididymis. *Fertil. Steril.* **28:**191–194
39. Wegman, E.A., Ishikawa, T., Young, J.A., Cook, D.I. 1992.

Cation channels in basolateral membranes of sheep parotid secretory cells. *Am. J. Physiol.* **263:**G786–G794

40. Wong, P.Y.D. 1988. Inhibition by chloride channel blockers of anion secretion in cultured epididymal epithelium and intact epididymis of rats. *J. Physiol.* **94:**155–163
41. Wong, P.Y.D. 1989. Potassium channel blockers inhibit anion secretion in cultured rat epididymal epithelium. *Jpn. J. Physiol.* **39:**595–607
42. Wong, P.Y.D. 1990. Electrolyte and fluid transport in the epididymis. *In:* Epithelial Secretion of Water and Electrolytes. P.Y.D. Wong and J.A. Young, editors. pp. 333–347. Springer Verlag, Heidelberg, Berlin
43. Wong, P.Y.D., Lee, W.M. 1983. Potassium movement during sodium-induced motility initiation in the rat cauda epididymal spermatozoa. *Biol. Reprod.* **28:**206–212
44. Wong, P.Y.D., Yeung, C.H. 1978. Absorptive and secretory functions of the perfused rat cauda epididymidis. *J. Physiol.* **275:**13–26